Journal of Magnetic Resonance **142,** 195–198 (2000)
Article ID jmre.1999.1961, available online at http://www.idealibrary.com on IDEAL®

COMMUNICATIONS

Three-Dimensional Protein NMR TROSY-Type ^{15}N-resolved $^{1}H^{N}$–$^{1}H^{N}$ NOESY Spectra with Diagonal Peak Suppression

Axel Meissner and Ole Winneche Sørensen

Department of Chemistry, Carlsberg Laboratory, Gamle Carlsberg Vej 10, DK-2500 Valby, Denmark

Received October 6, 1999; revised October 20, 1999

An earlier two-dimensional NOESY experiment with diagonal peak suppression in the $^{1}H^{N}$–$^{1}H^{N}$ region is extended to three dimensions by including ^{15}N evolution while maintaining the TROSY approach throughout. The technique suppresses all anti-TROSY resonances by appropriate pulse sequence elements and for large molecules at high fields possible semi- and anti-TROSY artifacts are further suppressed by virtue of much shorter transverse relaxation times for these components. The new technique is demonstrated using an ^{15}N-labeled protein sample, RAP 17-97 (N-terminal domain of α2-macroglobulin Receptor Associated Protein), in H_2O at 500 MHz.

Key Words: **diagonal peak suppression; TROSY; NOESY.**

Spin-state-selective (S^3) techniques make it possible to selectively manipulate the coherences belonging to particular states of passive spins and this can be applied for editing multidimensional NMR spectra, for example, allowing convenient measurement of coupling constants (*1–4*). Typically, a spin C is one-bond and long-range coupled to spins A and B, respectively, and the α and β spin states of C can be separated based on A-spin magnetization and this separation then maintained through a coherence transfer from spin A to spin B.

Another category of S^3 techniques is TROSY (*5*), where one particular 2D multiplet component having the most favorable transverse relaxation times is selected by an appropriate mixing sequence, thus resulting in a spectrum with enhanced resolution and sensitivity (*5, 6*). Such a 2D ^{1}H–^{15}N or ^{1}H–^{13}C peak corresponds to specific spin states of the attached passive spin, e.g., the ^{1}H-spin in the dimension of ^{15}N or ^{13}C, respectively. Moreover, it was recently shown that diagonal peak suppression is feasible based on the inherent pattern of spin-state selectivity associated with coherence transfer between two ^{1}H–^{15}N units (*7*). Specifically, when a TROSY coherence in one unit is partially transferred to another unit the result is equal amounts of TROSY and anti-TROSY coherence so that such a cross peak would be invariant to a π pulse applied on the attached heteronuclear passive spin. On the other hand, the coherence that is not transferred (i.e., the diagonal peak) is still associated with the TROSY transition so that a π pulse will transfer it to the anti-TROSY transition. As a result, a final selection of the TROSY resonances suppresses the diagonal (*7*) and apart from loss due to pulse imperfection and relaxation during extra delays there is no sensitivity penalty for molecules and field strengths sufficiently large to make the TROSY approach worthwhile.

In this communication, we extend the 2D NOESY pulse sequence with diagonal peak suppression (*7*) to three dimensions by including ^{15}N evolution. Such an ^{15}N-resolved NOESY spectrum is essential for evaluation of $^{1}H^{N}$–$^{1}H^{N}$ NOE cross peaks in larger proteins. The new ^{15}N-resolved TROSY NOESY experiment applies the TROSY approach in all three dimensions, something that is in contrast to a recent experiment and conclusions by Pervushin *et al.* (*8*). These authors suggest a 3D experiment with diagonal peak suppression involving ^{1}H–^{15}N zero-quantum coherence and apply it to a 110 kDa protein but show experimentally by 2D spectra that the single-quantum approach "clearly gives the best results" with respect to sensitivity and resolution. Nevertheless, it is argued that "the ZQ-based scheme is nonetheless a preferred element in 3D heteronuclear-resolved NOESY experiments" and that the potential advantage of the single-quantum based scheme "can hardly be exploited in 3D heteronuclear-resolved experiments (*8*)."

The pulse sequence for the new experiment is outlined in Fig. 1. It can be understood as the preparation sequence of the 2D NOESY pulse sequence with diagonal peak suppression in Ref. (*7*) having been replaced by the heteronuclear gradient echo TROSY sequence (*9, 10*) without the detection period, i.e., according to the regimen for constructing a 3D pulse sequence from two 2D sequences (*11*). The TROSY mixing sequence delivers the same result as the preparation sequence of the original 2D NOESY pulse sequence with diagonal peak suppression, namely selective excitation of the ^{1}H TROSY coherences in the evolution period preceding NOESY mixing. The anti-TROSY coherences are suppressed by the gradients selecting the heteronuclear gradient echoes between the two evolution periods.

In the 2D heteronuclear gradient echo TROSY sequence, only one coherence transfer pathway contributes in any given

1090-7807/00 $35.00

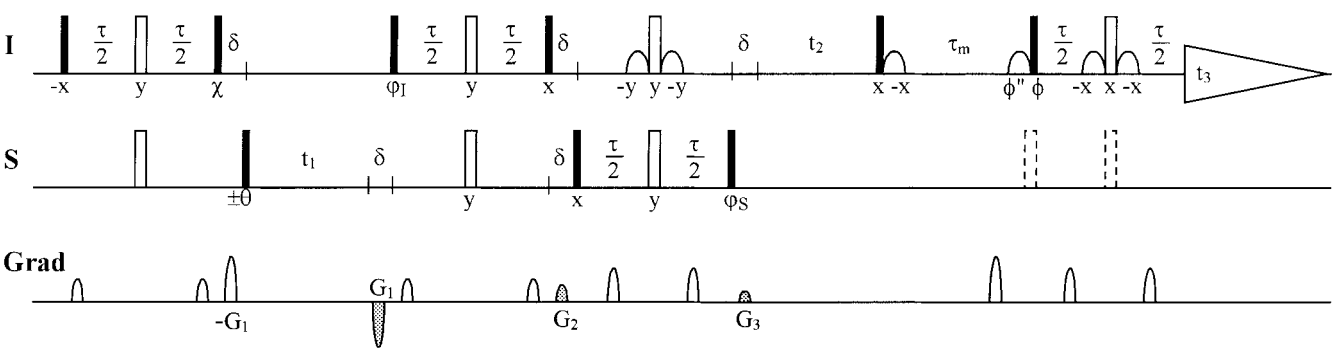

FIG. 1. 3D TROSY–NOESY pulse sequence with diagonal peak suppression. Filled and open bars represent $\pi/2$ and π pulses, respectively. Selective $\pi/2$ water pulses are shown as open bell shapes. $\tau = (2J_{NH})^{-1}$; δ is gradient delay; τ_m is NOESY mixing time. The phases are indicated below the pulses. For all odd-numbered scans the phase ϕ is x and the left dashed π pulse on the S channel is applied, while for all even-numbered scans ϕ is y and the right dashed π pulse on the S channel is applied with opposite receiver phase, $\phi'' = \phi + \pi$. To include the native ^{15}N (S-spin) magnetization in the TROSY coherence, the phase χ must be $-y$ on our Varian Unity Inova spectrometers, while it must be y for our Bruker DRX-600 instrument. The phases and selective water pulses ensure that the water magnetization is returned to the $+z$ axis. For ^{1}H and ^{15}N spins on our Varian spectrometers, the echoes between t_1 and t_2 are obtained with $\varphi_I = y$; $\varphi_S = y$, $G_1 = -7$, $G_2 = 3$, $G_3 = 2$, while for antiecho it is $\varphi_I = -y$; $\varphi_S = -y$, $G_1 = -8$, $G_2 = 2$, $G_3 = 3$. On the Bruker instrument φ_I and φ_S must be reversed. Apart from these gradients and the purge gradient during τ_m the pulsed field gradients are arranged in self-compensating pairs. Two data sets, A: $\{\theta = 0, \pi$; receiver $= 0, \pi\}$ and B: $\{\theta = \pi/2, 3\pi/2$; receiver $\pi/2, 3\pi/2\}$, both for echo (e) and antiecho (a) between t_1 and t_2, are recorded. The linear combinations {A(a) − B(a)}, {A(e) + B(e)}, {A(e) − B(e)}, and {A(a) + B(a)} yield the four pathways $\{S^-, S^+\}(t_1) \rightarrow \{I^-, I^+\}(t_2)$. This separation of the individual pathways offers the possibility to move the offset in F_2 to the middle of the amide region by TPPI-type preprocessing exponential multiplication of the individual FIDs. The t_2-dependent phase increments are of opposite sign for I^+ and I^-. By shifting the offset this way, the transmitter frequency can still remain on resonance for the water signal as is advantageous for water flip-back in TROSY type experiments (*15*).

scan, but in the 3D sequence there are two because both +1 and −1 quantum coherence in the second evolution period lead to observable signals. For example, the pathway $N^+ \rightarrow H^-$ in the 2D TROSY sequence is supplemented by $N^- \rightarrow H^+$ and that must be taken into account in the 3D Fourier transformation. The two relevant (φ_I, φ_S) phase settings in the TROSY

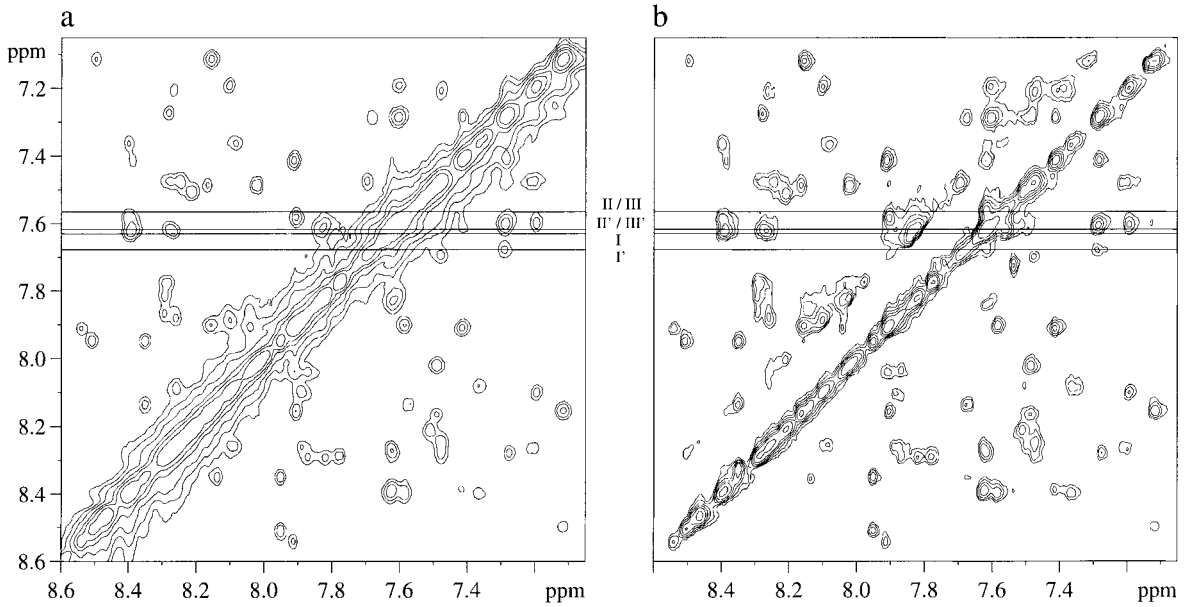

FIG. 2. Excerpts from the amide region of ^{15}N-labeled, RAP 17-97 (90% H_2O/10% D_2O, 25°C, pH 6.4, 20 mM NaCl, 1 mM phosphate buffer). (a) ^{15}N-edited 2D NOESY spectrum and (b) positive F_2/F_3 projection of the 3D TROSY–NOESY spectrum with diagonal peak suppression recorded with the pulse sequence in Fig. 1 on a Varian Unity Inova 500 MHz spectrometer. Parameters for (a): relaxation delay 1.5 s; $\tau = 5.26$ ms; $\tau_m = 100$ ms; t_1(max) = 61.72 ms; 16 scans. Sinc-shaped water pulses of duration 1.00 ms and Waltz-16 for ^{15}N decoupling during acquisition were applied. A data matrix of 864 × 2048 points covering 7000 × 7000 Hz were zero-filled to 2048 × 4096 points prior to States-TPPI Fourier transformation and the window functions were cosine in both dimensions. (b): relaxation delay 1.5 s; $\tau = 5.26$ ms; $\tau_m = 100$ ms; t_1(max) = 9.06 ms; t_2(max) = 61.72 ms; 16 scans. Sinc-shaped water pulses of duration 1.00 ms were applied. The data sets A and B were combined and the offset was shifted 1750 Hz in F_2 as described in the Fig. 1 caption. A data matrix of 16 × 432 × 2048 points covering 1655 × 3500 × 7000 Hz was zero-filled to 64 × 1024 × 4096 points prior to double echo/antiecho Fourier transformation and the window functions were cosine in F_3 and F_2 and cosine square in F_1. The excerpt from spectrum (b) is displaced by J/2 (48 Hz) in both dimensions to ease comparison.

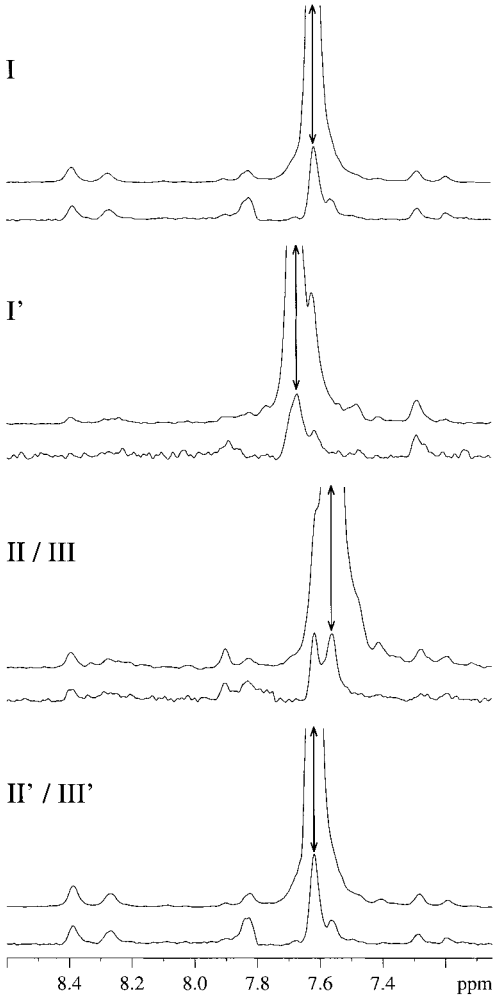

FIG. 3. Sections as indicated in Fig. 2 for three different $^{1}H^{N}$–$^{1}H^{N}$ pairs (I, II, and III). II and III cannot be separated in the 2D approach due to overlap. A double arrow marks the position of the diagonal. Sections marked with prime contain the high-frequency diagonal component of the amide pair, and sections without prime contain the low-frequency diagonal component. Top traces: sections from the spectrum in Fig. 2a without suppression of diagonal peaks; bottom traces: sections from the spectrum in Fig. 2b with diagonal peak suppression. Cross peaks close to the diagonal are clearly visible in the traces with diagonal peak suppression at places where they are hardly observable in the sections without diagonal peak suppression. Corresponding sections are scaled to show similar intensities for the cross peaks.

mixing sequence between t_1 and t_2 select $N^+ \rightarrow H^+$ and $N^- \rightarrow H^-$ or $N^+ \rightarrow H^-$ and $N^- \rightarrow H^+$, respectively. In practice, current spectrometer software can be used for Fourier transformation when these pairs of pathways are separated by a phase cycle of θ. Two data sets, ($\theta = 0$, π) and ($\theta = \pi/2$, $3\pi/2$), where the receiver phase in all cases is equal to θ, are recorded for each of the two (φ_I, φ_S) settings and they are added and subtracted, which results in four data sets that are Fourier transformed as so-called double echo/antiecho data. Another procedure is used in the ^{13}C–^{1}H–^{1}H TROSY–NOESY experiment of Brutscher *et al.* (*12*).

The new method for diagonal peak suppression in 3D TROSY–NOESY spectra was tested on an ^{15}N-labeled protein sample, RAP 17-97 (N-terminal domain of α2-macroglobulin Receptor Associated Protein) (*13*), using a Varian Unity Inova 500 MHz spectrometer. Figure 2 shows excerpts from the amide region of an ^{15}N-edited 2D ^{1}H–^{1}H NOESY spectrum employing Watergate (*14*) and ^{15}N decoupling throughout (Fig. 2a) and the positive F_2/F_3 projection from the 3D TROSY–NOESY spectrum with diagonal peak suppression (Fig. 2b) recorded using the pulse sequence in Fig. 1. Clearly, the latter shows a narrower and smaller diagonal with some nearby cross peaks that are obscured in the former. As demonstrated in Fig. 3 by sections taken at the points indicated by lines in Fig. 2, cross peaks that are submerged within the extension of the diagonal (indicated by double arrows) can be observed. The sections marked II/III and II′/III′ contain two overlapping signals, that are separated by the associated ^{15}N resonances in Fig. 4, where excerpts from selected F_2/F_3 planes and F_3 sections are shown. Inclined and horizontal dashed lines mark the diagonal and the F_3 sections, respectively. The cross to diagonal peak intensity ratios are typically even more favorable in 3D TROSY–NOESY spectra with diagonal peak suppression than in the corresponding 2D NOESY spectrum also employing diagonal peak suppression (*7*) because the spread according to ^{15}N chemical shifts in the third dimension reduces overlap on the diagonal.

In analogy to the earlier 2D NOESY experiment employing the same idea for diagonal peak suppression, the S^3E-type

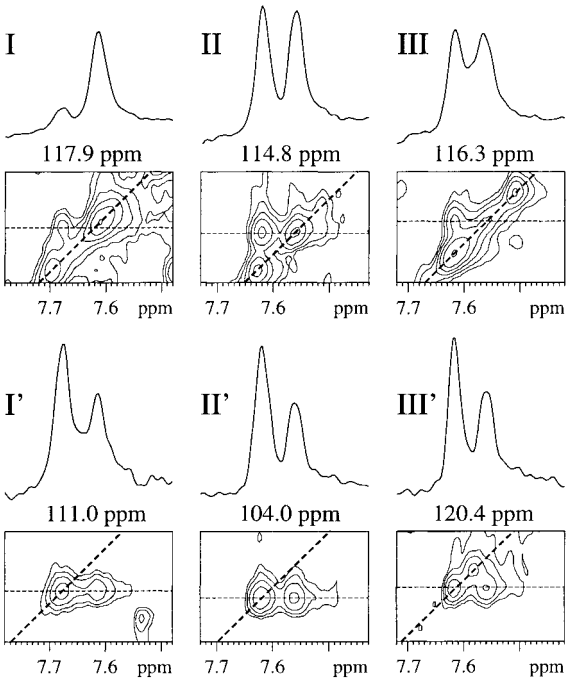

FIG. 4. F_2/F_3 excerpts from the 3D TROSY–NOESY spectrum with diagonal peak suppression for three different $^{1}H^{N}$–$^{1}H^{N}$ pairs (I, II, and III) as indicated in Fig. 2. The bold dashed lines mark the diagonal and the F_3 sections shown are taken at the positions of the thin dashed lines. ^{15}N chemical shifts in F_1 are given on top of the excerpts.

editing step prior to detection is not well compensated for variations in the J (and possibly residual dipolar) coupling constants and pulse imperfection, so artifacts are observed in the upper half of the spectrum in Fig. 2b at a distance of J from the diagonal in both dimensions. As such artifacts are not present in the lower half of the spectrum it is not worthwhile to extend the pulse sequence to improve the accuracy of this editing step. Furthermore, for large proteins at higher fields, where the TROSY approach is the one of choice for reasons of sensitivity and resolution, the artifacts are broadened beyond detection as they represent semi- and anti-TROSY peaks.

In conclusion, we have extended the 2D NOESY pulse sequence with diagonal peak suppression to three dimensions by replacing its preparation sequence by TROSY-type ^{15}N–^{1}H correlation. This pulse sequence will be valuable for application to larger proteins because of the improved effective resolution and because it is designed to take full advantage of the TROSY effect.

ACKNOWLEDGMENT

We thank Flemming M. Poulsen for the loan of the ^{15}N-RAP 17-97 sample.

REFERENCES

1. A. Meissner, J. Ø. Duus, and O. W. Sørensen, *J. Magn. Reson.* **128,** 92–97 (1997).
2. A. Meissner, J. Ø. Duus, and O. W. Sørensen, *J. Biomol. NMR* **10,** 89–94 (1997).
3. M. D. Sørensen, A. Meissner, and O. W. Sørensen, *J. Biomol. NMR* **10,** 181–186 (1997).
4. A. Meissner, T. Schulte-Herbrüggen, and O. W. Sørensen, *J. Am. Chem. Soc.* **120,** 3803–3804 (1998).
5. K. Pervushin, R. Riek, G. Wider, and K. Wüthrich, *Proc. Natl. Acad. Sci. U.S.A.* **94,** 12366–12371 (1997).
6. R. H. Griffey and A. G. Redfield, *Q. Rev. Biophys.* **19,** 51–82 (1987).
7. A. Meissner and O. W. Sørensen, *J. Magn. Reson.* **140,** 499–503 (1999).
8. K. Pervushin, G. Wider, R. Riek, and K. Wüthrich, *Proc. Natl. Acad. Sci. U.S.A.* **96,** 9607–9612 (1999).
9. A. Meissner, T. Schulte-Herbrüggen, J. Briand, and O. W. Sørensen, *Mol. Phys.* **95,** 1137–1142 (1998).
10. M. H. Lerche, A. Meissner, F. M. Poulsen, and O. W. Sørensen, *J. Magn. Reson.* **140,** 259–263 (1999).
11. C. Griesinger, O. W. Sørensen, and R. R. Ernst, *J. Magn. Reson.* **84,** 14–63 (1989).
12. B. Brutscher, J. Boisbouvier, A. Pardi, D. Marion, and J.-P. Simorre, *J. Am. Chem. Soc.* **120,** 11845–11851 (1998).
13. P. R. Nielsen, L. Ellgaard, M. Etzerodt, H. C. Thøgersen, and F. M. Poulsen, *Proc. Natl. Acad. Sci. U.S.A.* **94,** 7521–7525 (1997).
14. M. Piotto, V. Saudek, and V. Sklenar, *J. Biomol. NMR* **2,** 661–665 (1992).
15. M. Rance, J. P. Loria, and A. G. Palmer, III, *J. Magn. Reson.* **136,** 92–101 (1999).